Determination of the cyclic plastic zone using ECCI-Technique

Jürgen Bär

Universität der Bundeswehr München, Institut für Werkstoffkunde, D-85577 Neubiberg
Phone: ++49 89 6004-2561, fax: ++49 89 6004-3055, e-mail: juergen.baer@unibw.de

ABSTRACT. *The plastic zone around fatigue cracks in **O**xid **F**ree **H**igh **C**onductivity Copper and a high alloyed steel (X5CrNi18-10) was investigated with the ECCI-technique. The fatigue crack propagation experiments were undertaken under stress-intensity controlled conditions. In case of OFHC-Cu specimens typical cell-structures were observed close to the fatigue-crack. The X5CrNi18-10 specimens exhibit a fine fragmented structure close to the crack flanks. Beside this structure also slip-bands are visible. The size of the cyclic plastic zone can be easily measured by determining the extension of the area with the observed dislocation structure. Due to local differences in the grain size and orientation the scatter of the measured plastic zone sizes is very high. These results illustrate that the plastic zone and therewith the crack propagation behavior is influenced by the microstructure of the material.*

INTRODUCTION

The knowledge of the size of the plastic zone is an important fact for understanding the fatigue crack propagation in metallic materials. For the determination of the plastic zone size different methods, for example micro-hardness measurement [1], etching techniques [2] and many other have been used [3]. Most of these methods are inaccurate, take a great effort and are not suitable for small plastic zone sizes. The **E**lectron-**C**ontrast **C**hanneling-**I**maging technique allows a direct observation of the dislocation structure beneath a crack in a bulk material with a high resolution using a **S**canning **E**lectron **M**icroscope [4, 5]. In this work the dislocation structures beneath fatigue cracks and the size of the corresponding cyclic plastic zone is investigated for two different materials by ECCI-technique.

Experimental details

Material
The investigations were undertaken on OFHC-Copper and a stainless steel X5CrNi18-10 (AISI 304). The copper specimens were recrystallized for 2 h at 420°C. Figure 1 shows SEM-Images of the undeformed materials. In both materials the grains appear in different grey shades. In some grains twin boundaries are visible.
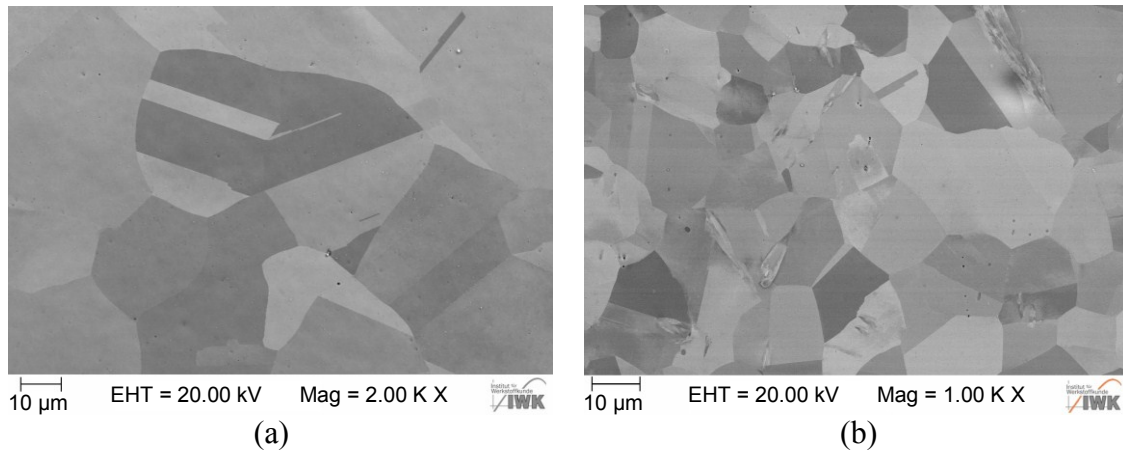
Figure 1. ECCI-Image of undeformed Copper (a) and X5CrNi18-10 (b).

Fatigue Crack propagation tests

The crack propagation experiments were undertaken on Single-Edge-Notch specimens with a size of 80 x 12 x 4 mm and a notch depth of 1 mm. The experiments were carried out under fully reversed loading conditions (R=-1) with a special equipped servohydraulic testing machine. Fixed grips were used to minimize bending forces. The crack length was measured online using a DC-potential drop method; therefore it was possible to perform the experiments with constant stress intensity, i.e. K_{max} = const and ΔK = const. A detailed description of the testing equipment has been reported in [6].
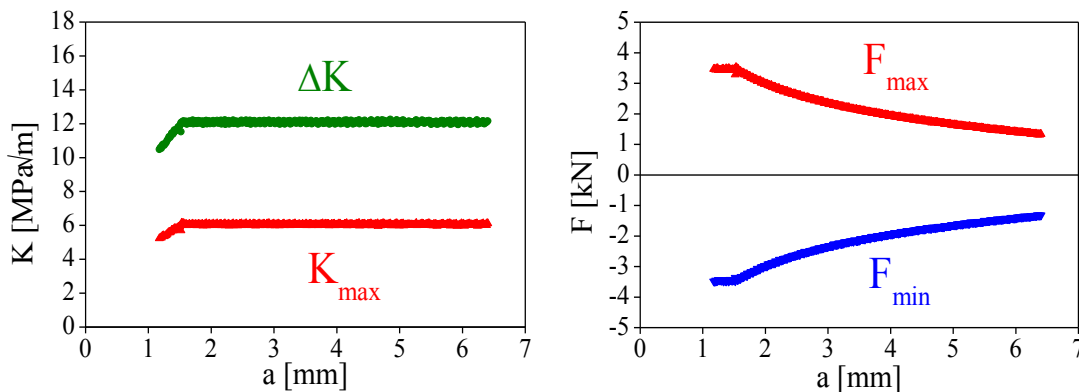

Figure 2. Stress-intensity and force during a crack propagation experiment on Copper.

In Figure 2 the stress intensity K_{max} and ΔK and the forces F_{max} and F_{min} achieved during a crack propagation experiment on Copper are plotted against the crack length. At the beginning of the experiment the force was kept constant and, consequently, the stress intensity increases with the crack length. Thereafter, the force was reduced with rising crack length to achieve constant stress intensity. The crack propagation experiment on copper was performed with a stress intensity of K_{max} = 6 MPa$\sqrt{m}$ and on

X5CrNi18-10 with a stress intensity of K_{max} = 11.5 MPa√m. The corresponding crack propagation rates were measured to be $5 \cdot 10^{-9}$ and 10^{-8} m/cycle, respectively.

ECCI-investigations

For the ECCI-investigations a Zeiss Ultra 55 field emission SEM was used. The images were made with an acceleration voltage of 20kV and a working distance of about 3 mm. For the ECC-Imaging the Angle-selective Backscattered electron-detector, a 4-quadrand BSE-detector which is mounted directly at the bottom of the final lens, was used. This equipment allows detecting differences in the crystallographic orientation and, therefore, grain-boundaries, twins as well as dislocation structures. A detailed description of the ECCI-contrast is given in [7].

Due to the fact that the ECCI-contrast is very weak, the specimens need a careful preparation to gain a flat and smooth surface. Consequently, the specimens have to be grinded and polished mechanically. To get an ideal surface all specimen have been electropolished, thereafter.

Results

OFHC-Copper

During cyclic loading in copper dislocations are forming a typical cell-structure as it has been found by many investigators [8, 9]. In figure 3 ECCI-images confirm these typical structures. Beside grain boundaries, cell structures are clearly visible. The orientation of the cells depends on the grain orientation and differs from grain to grain. The size of these cells is in the order of 1 – 3 µm.
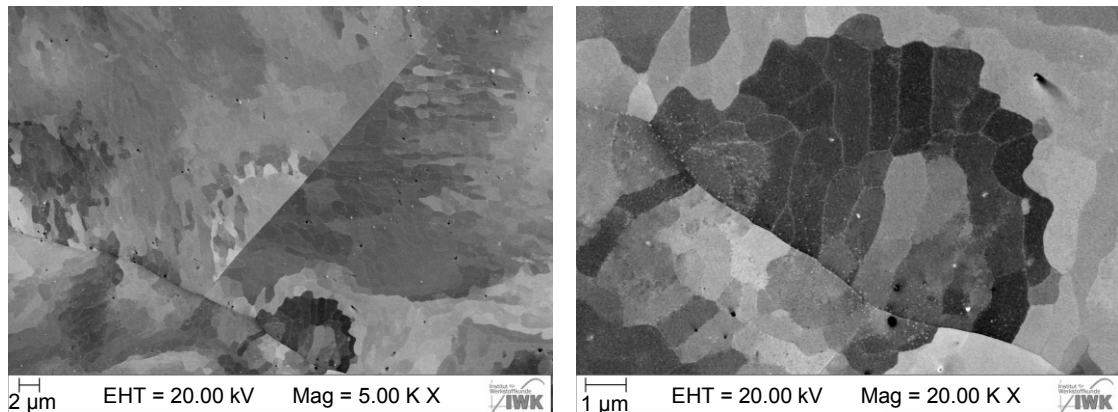
Figure 3. Cell-structure in fatigued OFHC-Copper.

In the vicinity of fatigue cracks, such a cell structure can be observed, too. The presence of the cell structure can be used to determine the size of the cyclic plastic zone. This is shown in figure 4 where the region in front of the crack tip, which shows such a cell structure, is bordered by a line.
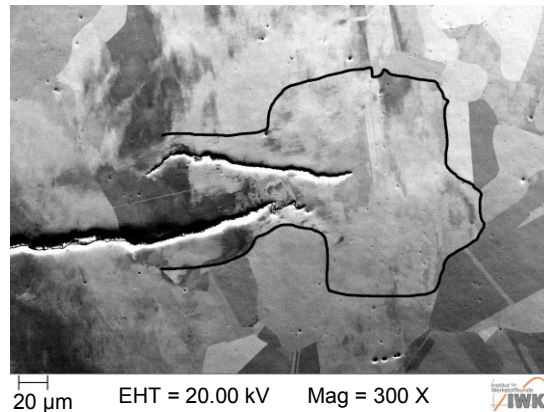
Figure 4. Cyclic plastic zone in OFHC-Copper bordered by a line.

To quantify the size of the cyclic plastic zone, the coordinates of its border are determined in relation to the crack tip by using an image analysis program. The Origin of the coordinate system was placed on the crack tip. The coordinates of the border were determined by setting points on the border of the region with a visible cell structure,.

To get information about the expansion of the plastic zone within the bulk, the specimen was grinded down in several steps and polished again prior to the ECCI investigation. The plastic zone size was determined in depth of 50, 150, 200, 300 and 750 μm, respectively, as it is shown in figure 5.
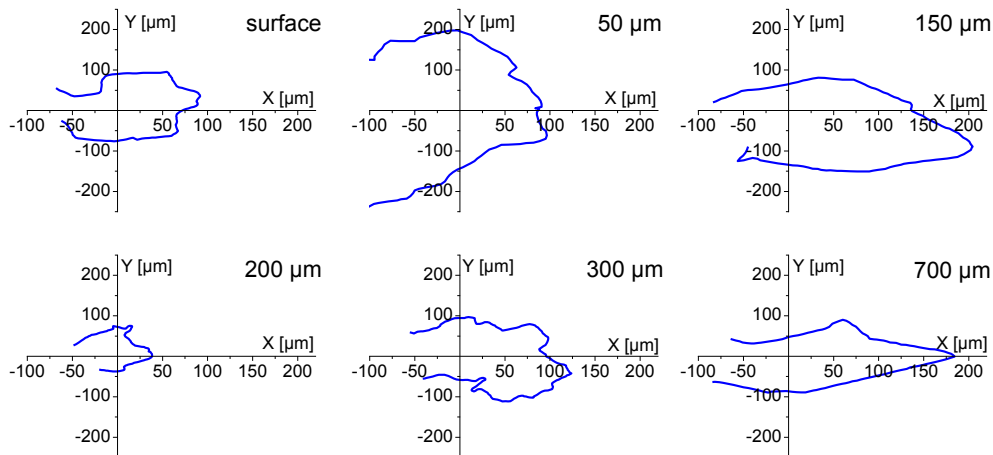

Figure 5. Plastic zone in OFHC-Copper in different depths.

Figure 5 demonstrates dramatic changes in the form and size of the plastic zone with increasing distance to the specimen surface. The size of the zone changes from slide to slide. As shown in table 1 no tendency in the plastic zone size with increasing depth is visible as it would be expected from continuum mechanical considerations. The maximum extension on the ligament (y=0) varies between 38 μm in a depth of 200μm and 183 μm in a distance of 700 μm to the surface.

Table 1. Size of the plastic zone on the ligament (y = 0)

Distance to surface	Size of the plastic zone
0 µm	72 µm
50 µm	87 µm
150 µm	136 µm
200 µm	38 µm
300 µm	96 µm
700 µm	183 µm
Mean value:	102 µm
Standard deviation:	51 µm

Stainless steel

In contrast to copper no distinct cell structure can be found in the stainless steel X5CrNi18-10. In the vicinity of a fatigue crack two different kinds of structures can be observed in the ECCI-images. As shown in figure 6 a fine fragmented structure is visible close to the crack. In a greater distance to the crack slip bands in different orientations are formed inside the grains. These slip bands that are obviously formed at lower stresses seem to be a kind of pre-stage of the fine fragmented structure. The latter may be caused by a martensitic transformation which is known to take place in this steel under monotonic loading [10]. To clarify this fact EBSD and x-ray measurements will be undertaken.

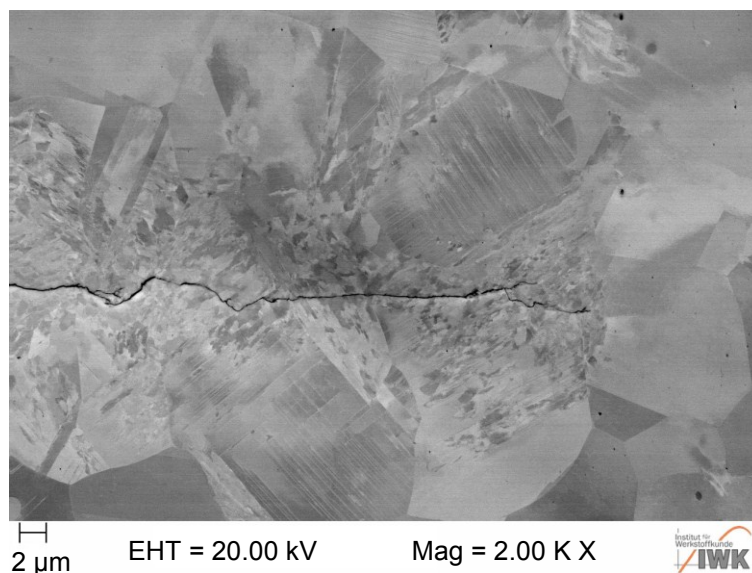2 µm   EHT = 20.00 kV   Mag = 2.00 K X

Figure 6. Structures around a fatigue crack in X5CrNi18-10.

To determine the size of the cyclic plastic zone it is necessary to define which kind of structure is within the cyclic plastic zone. Although slip bands are an indication for plastic deformation, the cyclic plastic zone was selected as the area with the fine fragmented structure.

To get more information the size of the cyclic plastic zone parallel to the loading direction was determined. The coordinates of the crack path and the rim of the cyclic plastic zone were determined using an image analysis program. In figure 7 the crosses and corresponding numbers represent the crack path and the border of the cyclic plastic zone for a fatigue crack in stainless steel.
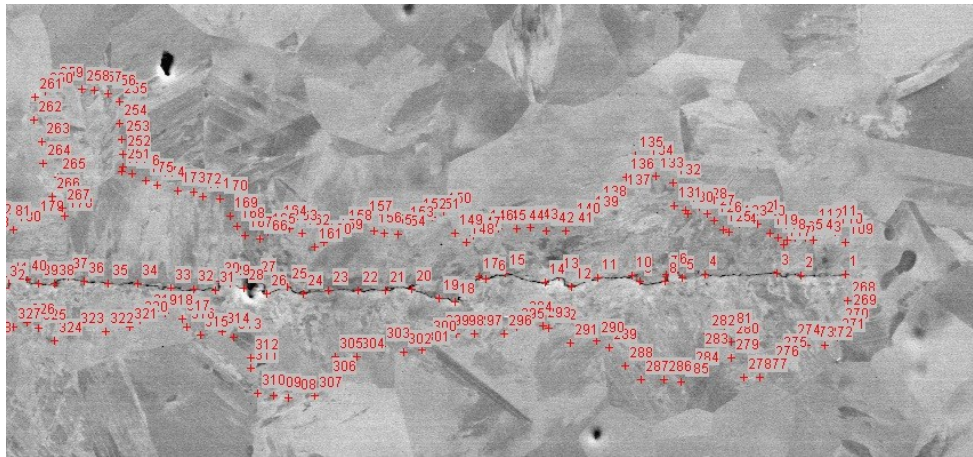

Figure 7. Determination of the plastic zone size in stainless steel.

In Figure 8 (a) both, the coordinates of the crack path (middle) and the border of the cyclic plastic zone are shown. To determine the size of the cyclic plastic zone the differences between the y-coordinates of the crack path and the border of the cyclic plastic zone were calculated. The result is shown in figure 8 (b).
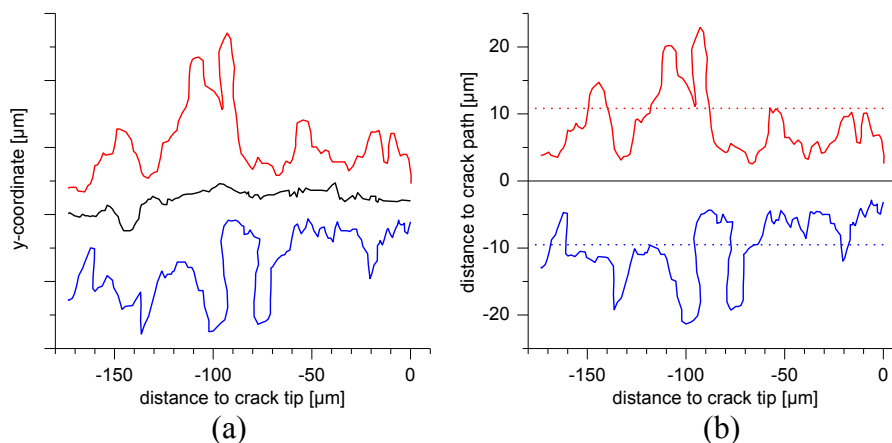

Figure 8. Determination of the plastic zone size in stainless steel.

To get information about the cyclic plastic zone within the bulk the specimen was grinded to different depths, polished and investigated in the SEM, respectively. In figure 9 the size of the cyclic plastic zone obtained in depths of 100 to 500 μm is shown. Similar to copper, great differences between the slides are visible. There is no indication for a trend that the size of the plastic zone decreases with the depth, too. In nearly all slides a great scatter of the size of the cyclic plastic zone is visible.
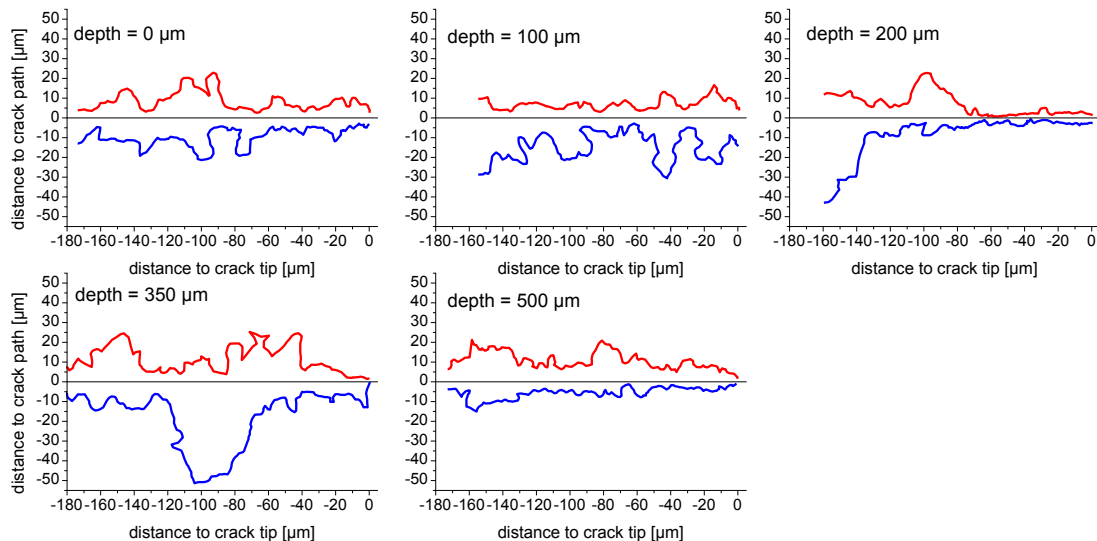

Figure 9. Determination of the plastic zone size in stainless steel.

DISCUSSION

The investigations on OFHC-Copper and stainless steel X5CrNi18-10 have shown that the ECCI-technique is a suitable method to investigate the dislocation structure beneath a fatigue crack. Consequently, this technique allows a direct measurement of the size of the cyclic plastic zone. In contrast to indirect methods, for example hardness measurement, the ECCI-technique allows a clear definition of the plastic zone based on the observed structure. Due to the high resolution in SEM-investigations, this method is also suitable for the investigation of small plastic zone sizes.

The results achieved on the two materials show a great scatter in the cyclic plastic zone size. In the case of OFHC-Copper this can be seen by the different sizes and forms of the dislocation structure that represents the plastic zone in different depths. In X5CrNi18-10 the plastic zone size should be constant with the crack length due to the constant stress intensity. With increasing depth a decreasing plastic zone size should be evident, when the change from plane stress to plane strain is taken into account. As the results clearly show, this decreasing size could not be observed. In fact the great scatter in the plastic zone sizes shows that the influence of the microstructure, especially the size and orientation of the grains determines the expansion of the cyclic plastic zone.

Therefore, all models to calculate the size of the cyclic plastic zone and the crack propagation rate based on continuum mechanics give solely a mean value but are not suitable to describe the local conditions. In case of thick specimens and high stress intensities and therefore great plastic zone sizes the mean value calculated by linear elastic fracture mechanics may give adequate values. For low stress intensities or thin samples the local conditions become relevant and, therefore, the size and orientation of the grains should be taken into account. For a comprehensive description of the size of the cyclic plastic zone a model that takes the microstructure into account is needed.

ECCI-investigations combined with crack propagation experiments with constant stress intensity and, therefore, constant loading conditions at the crack tip are suitable for the investigation of the cyclic plastic zone. Especially the measurement of the plastic zone size parallel to the loading direction provides a wide spectrum of data points within one specimen. Combined with EBSD-measurements to determine the orientation of the grains the data for a statistical model can be achieved with a couple of crack propagation experiments.

ACKNOWLEDGEMENT

REFERENCES

1. Nyström, M., Söderlund, E., Karlsson, B. (1995) *Int. J. Fatigue* **17**, 141-147.
2. Hahn, G.T., Hoagland, R.G., Rosenfield, A.R. (1972) *Met. Trans.* **3**, 1189-1202.
3. Uğuz, A., Martin, J.W. (1996) *Mat. Char.* **37**, 105-118.
4. Wilkinson, A.J., Henderson, M.B., Martin, J.W. (1996) *Phil. Mag. Let.* **74**, 145-151.
5. Kaneko, Y., Ishikawa, M., Hashimoto, S. (2005) *Mat. Sci. Eng.* **A400-401**, 418-421.
6. Bär, J., Volpp, T., (2001) *Materials Testing*, **43**, 242-247.
7. Wilkinson, A.J., Hirsch, P.B., (1997) *Micron* **28**, 279-308.
8. Laufer, E.E., Roberts, W.N. (1966) *Phil. Mag.* **14**, 65-78.
9. Lukáš, P., Klesnil, M., Krejči, J. (1968) *Phys. Stat. Sol.* (b) **27**, 545-558.
10. Rodríguez-Martínez, J.A., Pesci, R., Rusinek, A. (2011) *Mat. Sci. Eng.* **A528**, 5974-5982.